Trends in Renewable Energy
OPEN ACCESS ISSN:2376-2144
Peer-Reviewed Article futureenergysp.com/index.php/tre

Improvement of Power Systems Stability by Applying Topology Identification Methodology (TIM) and Fault and Instability Identification Methodology (FIIM) – Study of the Overhead Medium-Voltage Broadband over Power Lines (OV MV BPL) Networks Case

Athanasios G. Lazaropoulos[1]

1: School of Electrical and Computer Engineering / National Technical University of Athens / 9 IroonPolytechniou Street / Zografou, GR 15780

Received January 30, 2017; Accepted March 28, 2017; Published April 27, 2017

The performance of two useful piecewise monotonic data approximation (PMA) applications that are Topology Identification Methodology (TIM) and Fault and Instability Identification Methodology (FIIM) is investigated in this paper for the overhead medium-voltage broadband over power lines (OV MV BPL) networks. TIM and FIIM are applied to OV MV BPL networks when measurement differences, faults and instabilities occur. By exploiting the L1PMA optimal number of monotonic sections, advanced TIM and FIIM are also proposed and applied to OV MV BPL networks. The results of the four PMA applications are compared and it is found that advanced TIM and FIIM achieve higher computational speeds and almost equivalent identification performance in comparison with the respective original TIM and FIIM. Exploiting the better performance metrics of advanced TIM and FIIM, PMA applications provide a stable step towards the real time surveillance and monitoring of transmission and distribution power grid.

Keywords: Smart Grid; Intelligent Energy Systems; Broadband over Power Lines (BPL) Networks; Power Line Communications (PLC); Faults; Fault Analysis; Fault Identification and Prediction; Distribution Power Grids

1. Introduction

The power stability of transmission and distribution power grids relies on the increasing aging electrical grid systems worldwide, some of which originated from the earlies of 20th century. Nowadays, the power stability can be enhanced through the deployment of the broadband over powerlines (BPL) networks across this vintage power grid infrastructure. In fact, BPL technology can transform the traditional transmission and power grids into an integrated intelligent IP-based communications network with a myriad of smart grid applications [1]-[4].

In order to be able to deliver high-bandwidth applications (*e.g.*, HD video streaming and VoIP) with data rates that exceed 1Gbps, various inherent deficiencies of the BPL networks, such as the high and frequency-selective channel attenuation and noise, should be overcome now so that BPL networks can become both a

**Corresponding author:* AGLazaropoulos@gmail.com

Tr Ren Energy, 2017, Vol.3, No.2, 102-128. doi:10.17737/tre.2017.3.2.0034

useful power grid complement and a strong telecommunications competitor to the other wireless networking solution [5]-[13].

As the determination of the transfer functions of overhead medium-voltage (OV MV) BPL networks is concerned in this paper, the well-established hybrid method, which is employed to examine the behavior of various multiconductor transmission line (MTL) structures, is also adopted in this paper [5]-[9], [14]-[25]. Given as the inputs the OV MV BPL network topology, OV MV MTL configuration and the applied coupling scheme, the hybrid method gives as the output the corresponding transfer function.

Because of a number of practical reasons and "real-life" conditions, measurement differences between the experimental and theoretical results occur during the transfer function determination of OV MV BPL network topologies [2], [24]-[27]. To mitigate the aforementioned measurement differences and restore the theoretical BPL transfer function, piecewise monotonic data approximations (PMAs) have been successfully applied either in transmission or in distribution BPL networks [2], [24]-[27]. Among the available PMAs, L1PMA with optimal number of monotonic sections, which has been thoroughly analyzed and assessed in [2], [27], is proven to best approximate the theoretical OV MV BPL transfer functions regardless of the examined OV MV BPL network topology and the applied coupling scheme even if measurement differences ranging from 1 to 10dB are imposed.

On the basis of the aforementioned PMA benchmark results, two of the most useful PMA applications that are Topology Identification Methodology (TIM) of [24] and Fault and Instability Identification Methodology (FIIM) of [25] can be further upgraded. At first sight, TIM achieves to reveal the exact topological characteristics (*i.e.*, number of branches, length of branches, length of main lines and branch terminations) of a BPL topology by appropriately approximating the measured transfer function data, which are contaminated by measurement differences. TIM is based on the application of L1PMA. Through a similar L1PMA approximation of the measured transfer function data, FIIM achieves to identify faults and instabilities that occur in BPL topologies and can affect the power system stability. Although the performance of TIM and FIIM has been investigated in transmission BPL networks, these two PMA applications are first applied in distribution BPL networks, say OV MV BPL networks. Exploiting the optimal number of monotonic sections of [27], which offers better performance concerning the approximation efficiency of L1PMA, both TIM and FIIM can become more accurate and faster.

The rest of this paper is organized as follows: In Sec. II, the OV MV MTL configuration, the indicative OV MV BPL topologies and the basics of BPL signal transmission are presented. In Sec. III, a brief presentation of the L1PMA, TIM and FIIM is given as well as suitable performance metrics. Sec. IV discusses the simulations of various OV MV BPL networks intending to mark out the efficiency of TIM and FIIM in these networks as well as their performance upgrade due to the optimal number of monotonic sections. Sec. V concludes this paper.

2. Configurations, Topologies and BPL Signal Transmission

2.1 OV MV MTL Configuration

The OV MV MTL configuration, which is examined in this paper, is presented in Fig. 1(a) of [2]. This MTL configuration comprises three phase lines of radius $r_{\mathrm{MV,p}}$ that are spaced by Δ_{MV} and hung at typical heights h_{MV} above ground. The ground with conductivity σ_{g} and relative permittivity $\varepsilon_{\mathrm{rg}}$ is considered as the reference conductor. The exact values concerning the related conductor dimensions, ground properties and configuration geometry are reported in [5], [6], [17], [19], [21], [28]-[30]. The applied exact values define a realistic scenario during the following analysis while the impact of imperfect ground on broadband signal propagation via OV MV power lines was analyzed in [5], [6], [17], [19], [21], [31]-[33].

2.2 Indicative OV MV BPL Topologies

In accordance with [26] and with reference to Fig. 1(a), average path lengths of the order of 1000m are considered in OV MV BPL topologies. Four indicative OV MV BPL topologies, concerning end-to-end connections of average path lengths, are examined, namely:

1. A typical urban topology (OV MV urban case) with N=3 branches (L_1=500m, L_2=200m, L_3=100m, L_4=200m, L_{b1}=8m, L_{b2}=13m, L_{b3}=10m).
2. A typical suburban topology (OV MV suburban case) with N=2 branches (L_1=500m, L_2=400m, L_3=100m, L_{b1}=50m, L_{b2}=10m).
3. A typical rural topology (OV MV rural case) with only N=1 branch (L_1=600m, L_2=400m, L_{b1}=300m).
4. The "LOS" transmission along the same end-to-end distance L=L_1+…+L_{N+1}=1000m when no branches are encountered. This topology corresponds to Line of Sight transmission in wireless channels.

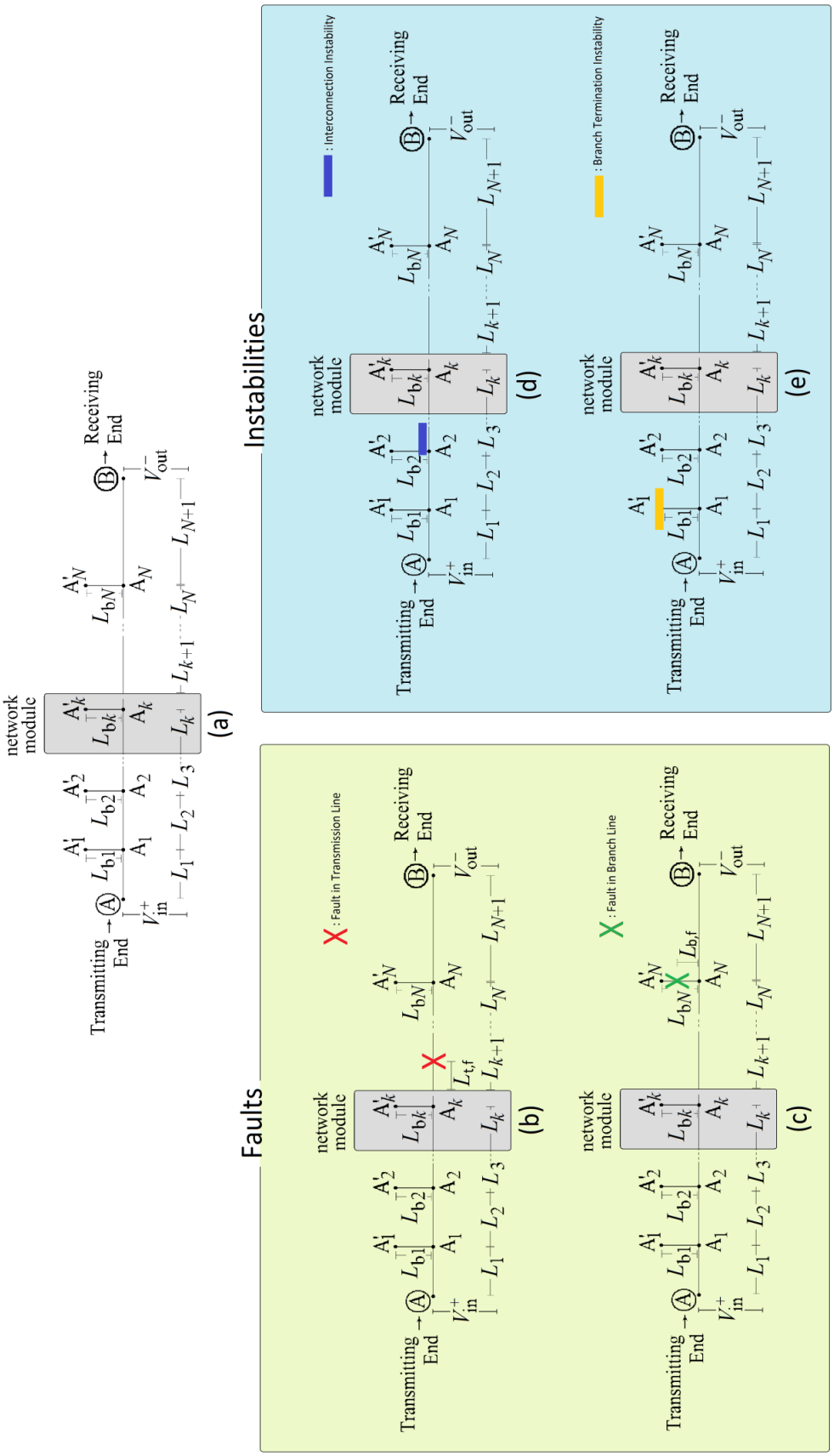

Figure 1. (a) General OV MV BPL topology [24]. (b, c) Faults in OV MV BPL topologies. (d, e) Instabilities in OV MV BPL topologies [25].

2.3 Hybrid Method, Coupling Schemes and Coupling Transfer Functions

Successfully tested in various transmission and distribution BPL networks [5]-[9], [14]-[23], [32]-[34], the well-established hybrid method consists of: (i) a bottom-up approach that is based on the MTL theory, eigenvalue decomposition (EVD) and singular value decomposition (SVD); and (ii) a top-down approach that is denoted as TM2 method and is based on the concatenation of multidimensional chain scattering matrices. Macroscopically, hybrid method gives as output the corresponding EVD modal and original transfer functions when the OV MV BPL network topology, OV MV MTL configuration and the applied coupling scheme are given as inputs.

Also, hybrid method may take as an input the way that the signals are injected into OV MV lines. In fact, two categories of coupling schemes are mainly supported by the OV MV BPL networks, namely [2], [16], [18], [24], [25], [35]-[37]: (i) Wire-to-Ground (WtG) coupling schemes; and (ii) Wire-to-Wire (WtW) coupling schemes. In the case of WtG coupling schemes, which is examined in this paper, the coupling WtG channel transfer function $H^{\mathrm{WtG^s}}\{\cdot\}$ is given from

$$H^{\mathrm{WtG^s}}\{\cdot\} = \left[\mathbf{C}^{\mathrm{WtG}}\right]^{\mathrm{T}} \cdot \mathbf{T}_V \cdot \mathbf{H}^{m}\{\cdot\} \cdot \mathbf{T}_V^{-1} \cdot \mathbf{C}^{\mathrm{WtG}} \quad (1)$$

where $\mathbf{C}^{\mathrm{WtG}}$ is an 3×1 coupling column vector with zero elements except in row *s* where the value is equal to 1, $\mathbf{T}_V$ is a $n^{\mathrm{OVMV}} \times n^{\mathrm{OVMV}}$ matrix that depends on the frequency, the OV MV MTL configuration and the physical properties of the cables and $\mathbf{H}^{\mathrm{m}}\{\cdot\}$ is the $n^{\mathrm{OVMV}} \times n^{\mathrm{OVMV}}$ EVD modal transfer function matrix that is given as an output by the hybrid method [5]-[9], [14]-[18], [21], [28], [38].

To give the coupling WtG channel transfer function of eq. (1), certain assumptions for the circuital parameters of OV MV BPL topologies need to be taken into account. In accordance with [2], these assumptions are: (i) The branch lines are assumed identical to the transmission ones; (ii) The interconnections between the transmission and branch conductors of the lines are fully activated; (iii) The transmitting and the receiving ends are assumed matched to the characteristic impedance of the modal channels; and (iv) The branch terminations are assumed open circuits.

3. L1PMA, TIM, FIIM and Performance Metrics

3.1 L1PMA

Various PMA methods have been proposed by Demetriou, such as L1PMA, L2WPMA and L2CXCV, that have been applied in transmission and distribution BPL networks so that the measurement differences can be mitigated and the theoretical OV MV BPL coupling transfer functions can be revealed [2], [24]-[27], [39]-[44]. Based on the comparative benchmark of the aforementioned PMA methods [26], [27], L1PMA has presented the higher and more stable overall mitigation performance against measurement differences and, for that reason, only L1PMA is applied in this paper.

In fact, L1PMA exploits the piecewise monotonicity property that always occurs in OV MV BPL coupling transfer functions. Analytically, L1PMA decomposes the coupling transfer functions into separate monotonous sections among their adjacent turning points (primary extrema) [41], [42]. Since the separate monotonous sections are identified, L1PMA separately handles them. As already been determined, the number of

monotonic sections can be equal either to the optimal number of monotonic sections, detailed in [2], [26], or to the adaptive number of monotonic sections, reported in [27]. According to [27], the adaptive number of monotonic sections helps towards the enhancement of the L1PMA mitigation performance against measurement differences; the concept of the adaptive number of monotonic sections is based on the need for more general approximations as the maximum differences increase and the examined OV MV BPL topologies increase in topological complexity.

On the basis of L1PMA and the adaptive number of monotonic sections, two of the most useful PMA applications that are TIM of [24] and FIIM of [25] can be further refined. Note that TIM and FIIM have been developed on the basis of L1PMA software, which receives as inputs the measured OV MV BPL coupling transfer function, the measurement frequencies and the number of monotonic sections and gives as output the best fit of the measured OV MV BPL coupling transfer function.

3.2 TIM, Advanced TIM and Curve Similarity Performance Metric (CSPM)

TIM is a PMA application that achieves to identify the real OV MV BPL topology by approximating and comparing the corresponding measured OV MV BPL coupling transfer function with a database of theoretical OV MV BPL coupling transfer functions. TIM consists of: (i) the hybrid method; (ii) L1PMA software; (iii) the OV MV BPL topology database; and (iv) CSPM that serves as the assessment metric of the TIM accuracy [24]. In accordance with [24], TIM CSPM achieves to reveal a set of candidate OV MV BPL topologies with the real topology lying inside it even though measurement differences of various distributions and magnitudes can occur.

More analytically, L1PMA gives the approximated OV MV coupling transfer function column vector $\overline{\overline{\mathbf{H}}}_{\text{meas}}^{\text{WtG}}(\mathbf{f},k_{\text{sect}})$ when measured OV MV one $\overline{\mathbf{H}}^{\text{WtG}}(\mathbf{f})$ and a number of monotonic sections k_{sect} are considered where $\mathbf{f}=\begin{bmatrix}f_1 & \cdots & f_i & \cdots & f_u\end{bmatrix}^{\text{T}}$ is the $u\times 1$ measurement frequency column vector. CSPM acts as the performance metric of the curve similarity between the measurement L1PMA approximation $\overline{\overline{\mathbf{H}}}_{\text{meas}}^{\text{WtG}}(\mathbf{f},k_{\text{sect}})$ and theory L1PMA approximation $\overline{\overline{\mathbf{H}}}_{\text{theor}}^{\text{WtG}}(\mathbf{f},k_{\text{sect}})$ and is determined by

$$CSPM_{k_{\text{sec}t}}\equiv CSPM_{k_{\text{sec}t}}\left(\overline{\mathbf{H}}^{\text{WtG}},k_{\text{sect}}\right)=\sum_{i=1}^{u}\left|\overline{\overline{\mathbf{H}}}_{\text{meas}}^{\text{WtG}}(f_i,k_{\text{sect}})-\overline{\overline{\mathbf{H}}}_{\text{theor}}^{\text{WtG}}(f_i,k_{\text{sect}})\right| \quad (2)$$

TIM is based on the CSPM and the OV MV BPL topology database in order to identify the OV MV BPL topology when a set of coupling transfer function measurements is available. TIM comprises three steps so that the OV MV BPL topology is revealed, say:

1. Given the measured OV MV BPL coupling transfer function column vector $\overline{\mathbf{H}}^{\text{WtG}}(\mathbf{f})$, the approximated OV MV BPL coupling transfer function column vector $\overline{\overline{\mathbf{H}}}_{\text{meas}}^{\text{WtG}}(\mathbf{f},k_{\text{sect}})$ is evaluated for monotonic sections that range from $k_{\text{sect,min}}$ to $k_{\text{sect,max}}$ where $k_{\text{sect,min}}$ and $k_{\text{sect,max}}$ is the minimum and maximum number of monotonic sections considered, respectively.

2. For each OV MV BPL topology and each monotonic section of the OV MV BPL topology database, the respective $CSPM_{k\text{sect}}$ of eq. (2) and the total $CSPM_{\text{tot}}$ are computed where

$$CSPM_{\text{tot}} \equiv \sum_{k_{\text{sect}}=k_{\text{sect,min}}}^{k_{\text{sect,max}}} CSPM_{k_{\text{sect}}} \tag{3}$$

3. TIM identifies OV MV BPL topologies with the lowest $CSPM_{\text{tot}}$ among all the available topologies of the database. These OV MV BPL topologies are members of the set of candidate OV MV BPL topologies. The number of candidate OV MV BPL topologies depends on the topological characteristics of the real topology (i.e., number of branches, branch length), the nature of measurement differences (i.e., measurement difference distributions, characteristics of distributions) and the number of monotonic sections.

In accordance with [24], TIM has been applied assuming that $k_{\text{sect,min}}$ and $k_{\text{sect,max}}$ are equal to 1 and 20, respectively, considering all the available L1PMA approximation cases. However, this assumption demands extremely high computational time, thus posing critical restrictions to the creation of the OV MV BPL topology database.

Taking into account the findings of [26], the adaptive number of monotonic sections can significantly reduce TIM computational load. Instead of considering the entire range of monotonic sections that ranges from 1 to 20, TIM analysis can only focus on a closed set of monotonic sections assuming that its set center $k_{\text{sect,AN}}$ is equal to the adaptive number of monotonic sections. Here, it should be noted that the adaptive number of monotonic section is unique given the examined OV MV BPL topology and an estimate of the magnitude of the occurred measurement differences. Numerically, $k_{\text{sect,min}}$ and $k_{\text{sect,max}}$ are assumed to be equal to

$$k_{\text{sect,min}} = \max\{1, k_{\text{sect,AN}} - 1\} \tag{4}$$

$$k_{\text{sect,max}} = \min\{20, k_{\text{sect,AN}} + 1\} \tag{5}$$

where $\max\{\cdot\}$ and $\min\{\cdot\}$ give the maximum and the minimum value among the examined values, respectively. Observing the bounds of the closed set of monotonic sections, this set consists of three or two values depending on the value of the set center $k_{\text{sect,AN}}$.

In average terms, the advanced TIM, which is based on eqs. (4) and (5), can achieve: (i) better accuracy performance during the identification of the real OV MV BPL topology since it considers only $CSPM_{k_{\text{sect}}}$ that can better approximate theoretical OV MV BPL coupling transfer functions; and (ii) reduction of the computational load that ranges from $100\% \cdot \frac{20-3}{20} = 85\%$ to $100\% \cdot \frac{20-2}{20} = 90\%$. The main disadvantage of the advanced TIM is that needs an estimate of the measurement difference condition in order to apply the suitable adaptive number of monotonic sections for given OV MV BPL topology.

3.3 FIIM, Advanced FIIM and Curve Similarity Performance percentage Metric (ΔCSPpM)

Apart from the aforementioned measurement differences during the determination of OV MV BPL coupling transfer functions, various serious problematic conditions can occur across the transmission and distribution power grids. FIIM identifies these problematic conditions that cause permanent damage to the power grid and their impact on the determination of OV MV BPL transfer functions totally change the form of the result.

In accordance with [25], FIIM repertory of faults and instabilities is presented in Figs. 1(b)-(e). In fact, the problematic conditions are divided into two categories with two subcategories each, namely:

- *Faults*: This category describes all the interruptions that can occur in the lines of a transmission power grid. There are two subcategories of line interruptions that are examined in this paper: (i) *Fault in transmission line* –see Fig. 1(b)–; and (ii) *Fault in branch line* –see Fig. 1(c)–.
- *Instabilities*: This category describes all the failures that can occur in the equipment across the transmission power grid. There are two subcategories of equipment failures that are examined in this paper: (i) *Instability in branch interconnections* –see Fig. 1(d)–; and (ii) *Instability in branch terminations* –see Fig. 1(e)–.

In total, FIIM can recognize either the fault or the instability condition and warn the responsible personnel.

As the implementation details of FIIM and its corresponding performance metrics are concerned, the proposed curve similarity performance percentage metric (ΔCSPpM), which acts as the accompanying performance metric of FIIM, is given by

$$\Delta CSPpM^{*} = CSPpM \ - CSPpM^{*} \tag{6}$$

where

$$CSPpM = 100\% \cdot \frac{\sum_{k_{\text{sect}}=k_{\text{sect,min}}}^{k_{\text{sect,max}}} \sum_{i=1}^{u} \frac{\left| \overline{\overline{\mathbf{H}}_{\text{meas}}^{\text{WtG}}}\left(f_i, k_{\text{sect}}\right) - \overline{\overline{\mathbf{H}}_{\text{theor}}^{\text{WtG}}}\left(f_i, k_{\text{sect}}\right) \right|}{\left| \overline{\overline{\mathbf{H}}_{\text{theor}}^{\text{WtG}}}\left(f_i, k_{\text{sect}}\right) \right|}}{\left(k_{\text{sect,max}} - k_{\text{sect,min}} + 1\right) \times u} \tag{7}$$

is retrieved during the normal operation of the OV MV BPL topology examined,

$$CSPpM^{*} = 100\% \cdot \frac{\sum_{k_{\text{sect}}=k_{\text{sect,min}}}^{k_{\text{sect,max}}} \sum_{i=1}^{u} \frac{\left| \overline{\overline{\mathbf{H}}_{\text{meas}}^{\text{WtG*}}}\left(f_i, k_{\text{sect}}\right) - \overline{\overline{\mathbf{H}}_{\text{theor}}^{\text{WtG}}}\left(f_i, k_{\text{sect}}\right) \right|}{\left| \overline{\overline{\mathbf{H}}_{\text{theor}}^{\text{WtG}}}\left(f_i, k_{\text{sect}}\right) \right|}}{\left(k_{\text{sect,max}} - k_{\text{sect,min}} + 1\right) \times u} \tag{8}$$

is retrieved during the problematic operation of the OV MV BPL topology when either fault or instability occurs and $\overline{\overline{\mathbf{H}}_{\text{meas}}^{\text{WtG*}}}\left(\mathbf{f}, k_{\text{sect}}\right)$ is the approximated measured OV MV BPL coupling transfer function column vector of the modified topology that comes from the application of L1PMA for different monotonic sections.

FIIM compares $\Delta CSPpM^*$ with a warning threshold $\Delta CSPpM_{\text{thr}}^*$ that is typically equal to zero. Details concerning the determination of the warning threshold $\Delta CSPpM_{\text{thr}}^*$ and the relative decisions are provided in [25].

Similarly to TIM, the adaptive number of monotonic sections can significantly enhance FIIM performance by taking into account the findings of [26]. Instead of considering the entire range of monotonic sections that ranges from 1 to 20, FIIM analysis can only focus on the closed set of monotonic sections defined in TIM case. By assuming set lower and upper bounds equal to $k_{\text{sect,min}}$ and $k_{\text{sect,max}}$, respectively. This advanced FIIM can achieve: (i) better accuracy performance during the identification of faults and instabilities since it considers only $CSPpM$ that can better approximate theoretical OV MV BPL coupling transfer functions; and (ii) reduction of the computational load that again ranges from 85% to 90%. The main disadvantage of the advanced FIIM is that needs an overall knowledge of the measurement difference environment in order to apply the suitable adaptive number of monotonic sections for given OV MV BPL topology.

4. Numerical Results and Discussion

4.1 Simulation Goals and Parameters

Various types of OV MV BPL topologies are simulated with the purpose of evaluating the proposed advanced TIM and FIIM against the original ones. In accordance with [24] and [25], the performance efficiency and the processing time of the advanced TIM and FIIM are assessed with regards to the indicative OV MV BPL topologies and the nature of the occurred measurement differences. Actually, measurement differences that occur in OV MV BPL networks are typically described by CUD with maximum CUD value that is equal to α_{CUD}.

As regards the hybrid method and L1PMA with adaptive number specifications, those are the same with [24]. More specifically, the BPL frequency range and the flat-fading subchannel frequency spacing are assumed equal to 1-30MHz and 1MHz, respectively. Therefore, the number of subchannels u in the examined frequency range is equal to 30. Arbitrarily, the WtG[1] coupling scheme is applied during the following simulations. Finally, the maximum number of monotonic sections $k_{\text{sect,max}}$ that is going to be used is assumed to be equal to 20 [2].

As the OV MV BPL topology database specifications are concerned, the maximum number of branches N, the length spacing L_{s} for both branch distance and branch length and the maximum branch length L_{b} are assumed equal to 2, 50m and 300m, respectively.

4.2 L1PMA with Adaptive Number of Monotonic Sections

The advanced TIM and FIIM are both based on the concept of the adaptive number of monotonic sections, which has been presented in [27]. To compute the adaptive number of monotonic sections, an estimation of the maximum CUD value, which occurs during the operation of OV MV BPL network, is required. In fact, the adaptive number of monotonic sections comes from the monotonic section

localization of the best measurement difference mitigation performance given the maximum CUD value, the examined OV MV BPL topology and the applied WtG coupling scheme. Already been reported in [27], the adaptive number of monotonic sections for the indicative OV MV BPL topologies of Sec.2.2 is presented in Table 1 when WtG[1] coupling scheme is applied and maximum CUD value range from 0 to 10dB. Also, the lower and upper bounds of the monotonic section set, which are reported in eqs. (4) and (5) and are going to be used in advanced TIM and FIIM of the following subsections, are presented in each of the cases examined.

From Table 1, it is evident that the adaptive number of monotonic sections decreases as the maximum CUD value increases for given OV MV BPL topology. This is a reasonable result since there is need for more general approximations as the measurement differences create significant differences between theoretical and measured OV MV BPL coupling transfer functions. Towards that direction, the lower and upper bounds of monotonic section sets follow this trend. Anyway, the narrow monotonic section sets allow to avoid large values of $CSPM_{ksect}$ that little contribute to the overall CSPM and CSPpM performance of TIM and FIIM, respectively.

Since OV MV BPL coupling transfer functions present close behavior for given number of branches [19], [20], [33], [38], the adaptive number of monotonic sections of urban, suburban, rural and "LOS" case, which is reported in Table 1, can characterize all the OV MV BPL topologies of 3, 2, 1 and 0 branches, respectively. This latter observation is used during the following analysis.

4.3 Performance of TIM and Advanced TIM

Prior to apply TIM and advanced TIM, a preliminary task is the preparation of the required OV MV BPL topology database in each case. The two OV MV BPL topology databases comprise all the possible topological configurations of OV MV BPL topologies concerning the number of branches, each branch distance from the transmitting end, each branch length and the required number of monotonic sections. Taking under consideration the topology database specifications of [24] and Table 1, the size requirements of the OV MV BPL topology databases are:

- ($k_{sect,max}$ - $k_{sect,min}$ + 1) approximated theoretical OV MV BPL coupling transfer function column vectors per each possible OV MV BPL topology of the database, which corresponds to the respective ($k_{sect,max}$ - $k_{sect,min}$ + 1) monotonic sections.
- 30 elements per each approximated theoretical OV MV BPL coupling transfer function column vector, which corresponds to the respective 30 measurement frequencies.
- When N branches are considered across the "LOS" transmission path, there are

$$\sum_{i_1=1}^{L/L_s+1}\left\{\sum_{i_2=1}^{i_1}\left\{\cdots\sum_{i_{N-1}=1}^{i_{N-2}}\left\{i_{N-1}\right\}\right\}\right\}\times\left(\frac{L_b}{L_s}+1\right)^N \tag{9}$$

possible OV MV BPL topologies that should be inserted in the OV MV BPL topology databases.

TABLE 1
Adaptive Number of Monotonic Sections of [27] and Monotonic Section Sets for the Indicative OV MV BPL Topologies when Different Maximum CUD Values Are Applied

Indicative OV MV BPL Topology	Maximum CUD Value	L1PMA		Advanced TIM and FIIM	
		Adaptive Number of Monotonic Sections	Cardinality of the Monotonic Section Set ($k_{\mathrm{sec}t,\max} - k_{\mathrm{sec}t,\min} + 1$)	Monotonic Section Set [$k_{\mathrm{sect,min}}$ $k_{\mathrm{sect,max}}$]	Cardinality of the Monotonic Section Set ($k_{\mathrm{sec}t,\max} - k_{\mathrm{sec}t,\min} + 1$)
Urban	0	12	20	[11 13]	3
	1	8	20	[7 9]	3
	2	10	20	[9 11]	3
	3	8	20	[7 9]	3
	4	10	20	[9 11]	3
	5	8	20	[7 9]	3
	6	8	20	[7 9]	3
	7	8	20	[7 9]	3
	8	8	20	[7 9]	3
	9	8	20	[7 9]	3
	10	4	20	[3 5]	3
Suburban	0	20	20	[19 20]	2
	1	16	20	[15 17]	3
	2	6	20	[5 7]	3
	3	18	20	[17 19]	3
	4	4	20	[3 5]	3
	5	10	20	[9 11]	3
	6	4	20	[3 5]	3
	7	4	20	[3 5]	3
	8	4	20	[3 5]	3
	9	4	20	[3 5]	3
	10	1	20	[1 2]	2
Rural	0	6	20	[5 7]	3
	1	6	20	[5 7]	3
	2	2	20	[1 3]	3
	3	2	20	[1 3]	3
	4	2	20	[1 3]	3
	5	1	20	[1 2]	2
	6	1	20	[1 2]	2
	7	2	20	[1 3]	3
	8	1	20	[1 2]	2
	9	1	20	[1 2]	2
	10	1	20	[1 2]	2
“LOS”	0	6	20	[5 7]	3
	1	6	20	[5 7]	3
	2	2	20	[1 3]	3
	3	2	20	[1 3]	3

	4	2	20	[1 3]	3
	5	2	20	[1 3]	3
	6	1	20	[1 2]	2
	7	2	20	[1 3]	3
	8	1	20	[1 2]	2
	9	1	20	[1 2]	2
	10	1	20	[1 2]	2

Taking under consideration the previous requirements, the OV MV BPL topology database specifications of Sec.4.1 and eq.(1) of [24], there are $\sum_{i_1=1}^{21}\left\{\sum_{i_2=1}^{i_1}\left\{\cdots\sum_{i_{N-1}=1}^{i_{N-2}}\{i_{N-1}\}\right\}\right\}\times 7^N\times \text{card}\left(k_{\text{sec}t,\max}-k_{\text{sec}t,\min}+1,0\right)\times 30$ elements required to be inserted in the database where $\text{card}\left(k_{\text{sec}t,\max}-k_{\text{sec}t,\min}+1,a_{CUD}\right)$ computes the cardinality of the monotonic section set when the maximum CUD value is equal to α_{CUD}. Recognizing the dependence of the number of elements on the term ($k_{\text{sect,max}}$ - $k_{\text{sect,min}}$ + 1), the size decrease of the advanced TIM database may reach up to 90%.

Numerically, the number of elements and the approximated time duration of inserting all the available OV MV BPL topologies for a specific number of branches is reported in Table 2 when the TIM and advanced TIM databases are created. Note that the system technical characteristics of [24] are assumed so that an approximation time duration can be delivered.

Already been reported in [24], it is also evident from Table 2 that the approximated time duration poses significant technical difficulties during the consideration of OV MV BPL topologies with high number of branches in the database regardless of the method applied, say either TIM or advanced TIM. However, the time reduction that is offered by the advanced TIM is significant even from the two-branch OV MV BPL topologies. Anyway, advanced TIM is the first step of the future research towards the need for the optimization of the insertion methodology in topology database is among the critical steps of the future research [24], [25]. Similarly to [24], only the cases of "LOS" case and topologies with one branch are considered during the comparison between TIM and advanced TIM for the sake of simplicity and speed (see Sec.VE).

Since the OV MV BPL topology databases are available, TIM and advanced TIM can now be applied if the three steps of Sec.3.2 are followed, namely:

1. The measured OV MV BPL coupling transfer function column vector $\overline{\mathbf{H}^{\text{WtG}}}(\mathbf{f})$ and the approximated OV MV BPL coupling transfer function column vector $\overline{\overline{\mathbf{H}_{\text{meas}}^{\text{WtG}}}}\left(\mathbf{f},k_{\text{sect}}\right)$ are computed for different number of monotonic sections as reported in Table 1 for TIM and advanced TIM (see the column of the cardinality of the monotonic section set).

TABLE 2
Number of OV MV BPL Topologies, Elements and Approximated Time Duration of Topology Databases

Number of Branches	Number of Topologies	TIM		Advanced TIM		Time Reduction (%)
		Number of Elements	Approximated Time Duration (hours)	Number of Elements	Approximated Time Duration (hours)	
0	1	600	0.003	90	0.0005	83.33
1	147	92,610	0.50	13,230	0.07	85.71
2	11,319	7,130,970	38.43	679,140	3.66	90.48
3	607,453	382,695,390	2062	54,670,770	294.61	85.71

2. With reference to eq. (3), the OV MV BPL topology database and the approximated measured OV MV BPL coupling transfer functions, the $CSPM_{tot}$ of the indicative topologies is calculated with respect to the topologies of the database. In Fig. 2(a), the $CSPM_{tot}$ of the indicative rural OV MV BPL topology is plotted versus the maximum CUD value a_{CUD} for TIM and advanced TIM. In Fig. 2(b), the position among the 1 + 147 = 148 OV MV BPL topologies of the database in ascending $CSPM_{tot}$ order is plotted versus the maximum CUD value a_{CUD} for TIM and advanced TIM when the indicative rural case is examined. In Fig. 3(a) and 3(b), similar curves with Figs. 2(a) and 2(b) are presented, respectively, but for the indicative "LOS" topology.
3. A set of candidate OV MV BPL topologies with their respective $CSPM_{tot}$ is provided by the TIM and advanced TIM as it is shown in Figs. 2(b) and 3(b). All these topologies present the same $CSPM_{tot}$ and coincide at the first position in ascending $CSPM_{tot}$ order.

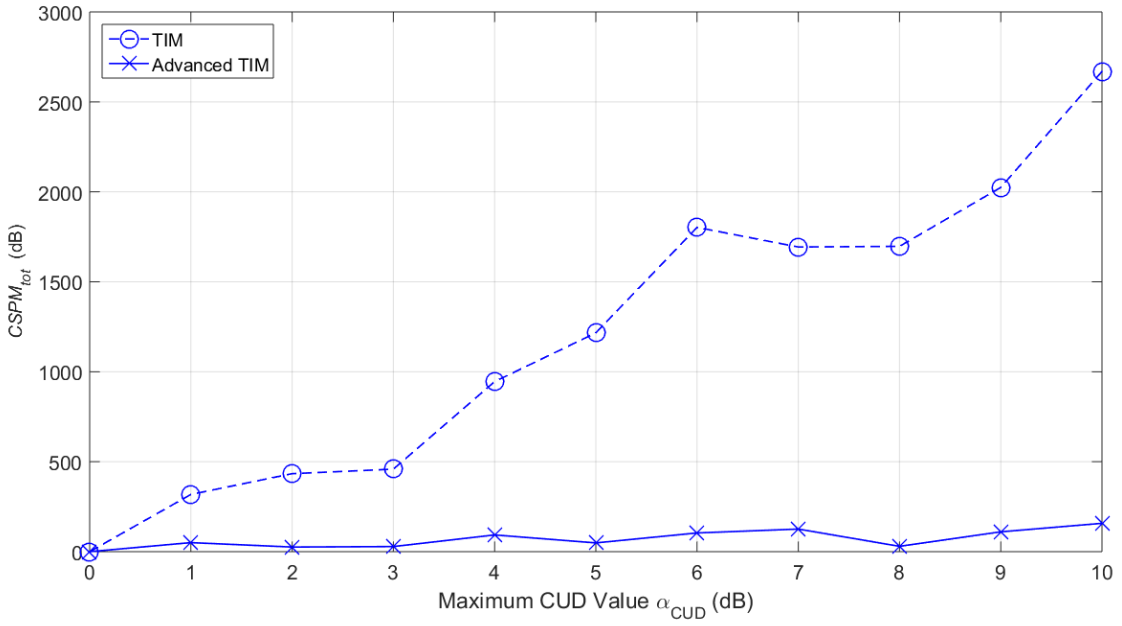

(a)

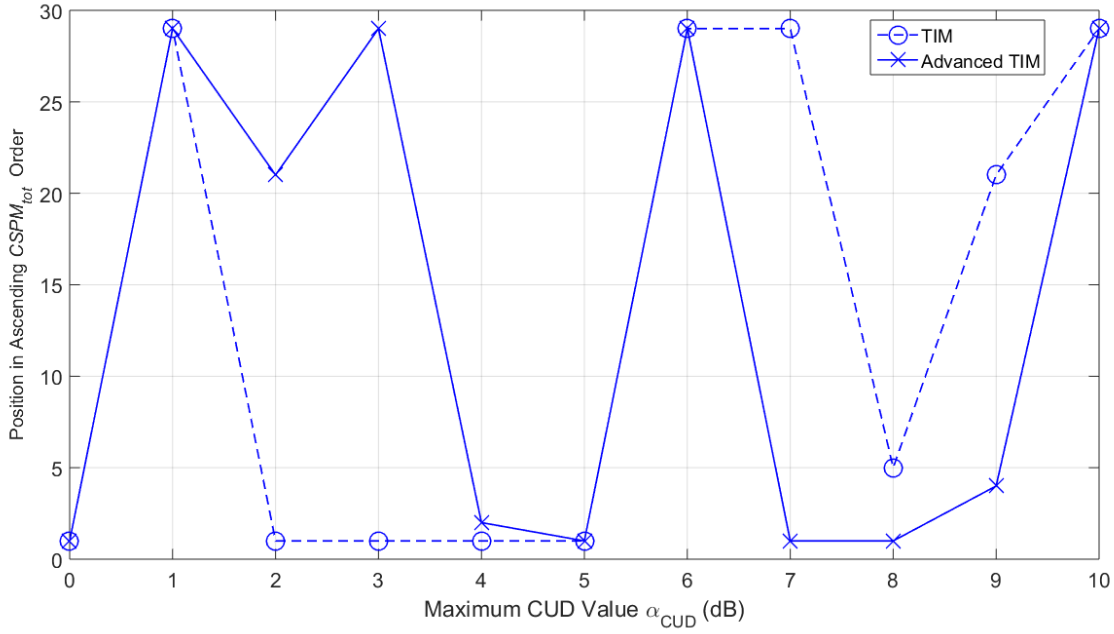

(b)

Figure 2. $CSPM_{tot}$ and position in ascending $CSPM_{tot}$ order versus maximum CUD value when TIM (⊖) and advanced TIM (✕) are applied in indicative rural case.

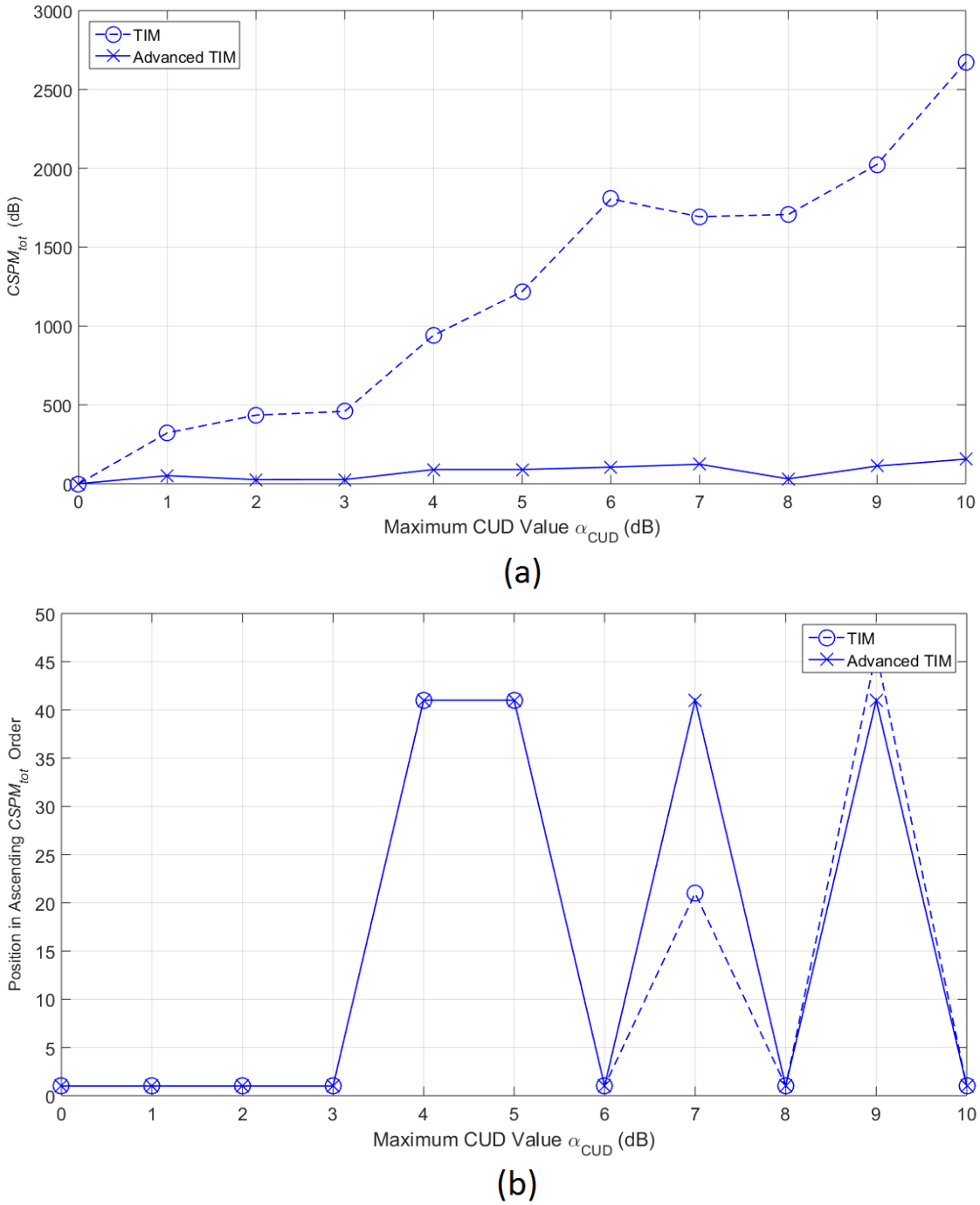

Figure 3. Same with Figure 2 but for the indicative "LOS" case.

From Figs. 2(a), 2(b), 3(a) and 3(b), several interesting observations concerning the performance of TIM and advanced TIM can be pointed out:

- Comparing the aforementioned figures with Figs. 5(a)-(d) of [24], it is shown that TIM efficiently copes with either OV HV BPL topologies or OV MV BPL ones. This is due to the fact that the poor multipath transmission environment of OV HV BPL networks has as a result the presence of coupling transfer functions that present great similarities each other, thus, creating a great set of candidate OV HV

BPL topologies. In contrast, the set of candidate OV MV BPL topologies comprises fewer elements and significant position fluctuations may occur.

- Both TIM and advanced TIM satisfactorily identify the real OV MV BPL topology even if maximum CUD values that reach up to 10dB are assumed. In accordance with [24], the identification performance of TIM and advanced TIM is significantly higher than the respective one of the traditional identification methods that focus on the comparison of the measured OV MV BPL coupling transfer function data with the theoretical ones. Anyway, TIM seems to better identify the real OV MV BPL topologies when low maximum CUD values occur whereas advanced TIM has better identification performance when high maximum CUD values occur.
- Similarly to [24], $CSPM_{tot}$ values of TIM define the accuracy of the topology identification. In fact, higher values of $CSPM_{tot}$ imply that topologies of either rich multipath environment or strongly contaminated by measurement differences are examined while $CSPM_{tot}$ difference between the candidate OV MV BPL topologies of the set and the first topology outside the set decreases. Here, a mask of secure topology identification can be defined that mainly depends on the examined OV MV BPL topology and maximum CUD value. Anyway, this mask is easily applicable to TIM because of its higher $CSPM_{tot}$ values.
- Since an OV MV BPL topology can be almost uniquely identified by the form of $CSPM_{tot}$ against various maximum CUD values, significant $CSPM_{tot}$ deviations that occur during the operation of an OV MV BPL topology imply that either a fault or instability may be arisen. This is the conceptual basis for FIIM of [25] so that faults or instabilities across an intelligent energy system can be identified.
- In order to further compare advanced TIM against TIM, the number of OV MV BPL topologies, elements and approximated time duration that are required to create the topology databases of advanced TIM and TIM are reported in Table 2. Although TIM and advanced TIM present approximately the same performance to identify an OV MV BPL topology from the respective database –see Figs. 2(a), 2(b), 3(a) and 3(b)–, the time reduction during the creation of the OV MV BPL topology database that is gained by the advanced TIM application is significant –see the respective columns of Approximated Time Duration in Table 2–.

4.4 Performance of FIIM and Advanced FIIM

As already been reported in Sec. 3.3, FIIM and advanced FIIM can identify four problematic conditions when these occur in OV MV BPL topologies, namely: (i) *Fault in main distribution lines*; (ii) *Fault in branch lines*; (iii) *Instability in branch interconnections* –see Fig. 1(d)–; and (iv) *Instability in branch terminations* –see Fig. 1(e)–. In total, FIIMs can recognize either the fault or the instability condition and warn the responsible personnel. OV MV BPL topologies that suffer from faults or instabilities are treated as modified OV MV BPL topologies and characterized by new respective OV MV BPL coupling transfer functions and measurement differences.

4.4.1 Fault in Main Distribution Line

As a fault in main distribution lines is assumed, an immediate communications failure in the OV MV BPL topology occurs. If transmitting and receiving ends operate in

stable conditions then a warning of fault in main distribution line is issued to the responsible personnel.

4.4.2 Fault in Branch Line

In accordance with [25], a fault in branch lines implies that a branch line is interrupted and an open circuit at the fault occurs. With reference to Fig. 1(c), let the first branch of each indicative OV MV BPL topology be broken at 2m from the branching interconnection A_1 with the main distribution line. The modified OV MV BPL topology is characterized by more frequent and deeper spectral notches due to the fact that a new shorter branch creates a richer multipath environment. In Fig. 4(a), FIIM CSPpM of the original urban OV MV BPL topology, FIIM CSPpM* of the modified urban OV MV BPL topology and their FIIM $\Delta CSPpM^*$ are plotted versus the maximum CUD value of the occurred measurement differences, which is assumed to be common for the two applied CUDs. Similar curves with Fig. 4(a) are given in Fig. 4(b) but for the application of the advanced FIIM. Similar curves with Figs. 4(a) and 4(b) are given in Figs. 4(c) and 4(d) for the suburban case and in Figs. 4(e) and 4(f) for the rural case.

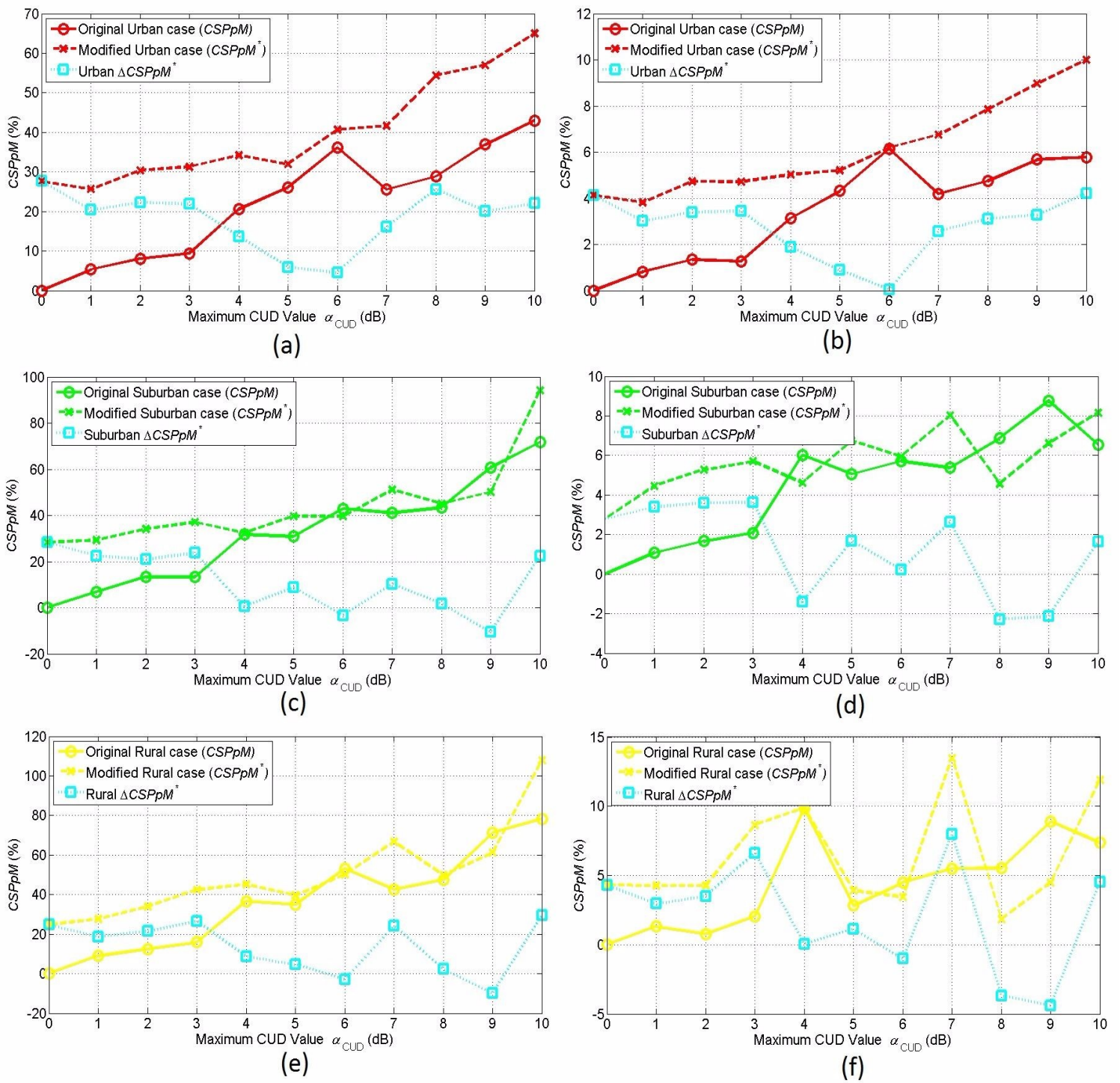

Figure 4. Fault in the first branch of the indicative OV MV BPL topologies and the behavior of CSPpMs and ΔCSPpM*. (a) FIIM / Urban case. (b) Advanced FIIM / Urban case. (c) FIIM / Suburban case. (d) Advanced FIIM / Suburban case. (e) FIIM / Rural case. (f) Advanced FIIM / Rural case.

From Figs. 4(a)-(f), it is evident that OV MV BPL topologies that suffer from a fault in their branch lines are characterized by modified OV MV BPL coupling transfer functions that differ from the original ones. These differences are reflected on CSPM*

and CSPM, respectively. Especially, the difference, which is expressed by the respective ΔCSPpM curves, is easily observable when measurement differences remain relatively low. As the measurement differences increase, measurement differences become important affecting the original form of the OV MV BPL coupling transfer functions and the identification potential of branch faults. Although the accuracy of FIIM and advanced FIIM to identify the faults in branch lines remains almost the same, advanced FIIM presents better computational speed in comparison with FIIM. However, both methods fail to identify faults of high maximum CUD value when these faults occur in OV MV BPL topologies of low branch complexity –e.g., see Figs. 4(e)-(f) when the maximum CUD value is equal to 8 or 9dB–.

4.4.3 Instability in Branch Interconnection

Branch interconnections connect main lines with branch ones and establish the stable power flow till the MV/LV transformers. In this section, the performance of FIIM and advanced FIIM to identify instabilities that occurs in a branch interconnection is investigated in this subsection. With reference to Fig. 1(d), the interruption of the last branch at the point A_N cancels the presence of this branch. The modified (N-1)-branch OV MV BPL topology comes from the original N-branch one.

Similarly to branch line faults, in Fig. 5(a), CSPpM of the original urban OV MV BPL topology, CSPpM* of the modified urban OV MV BPL topology and their $\Delta CSPpM^*$s are plotted versus the CUD maximum value of the occurred measurement differences when FIIM is applied. Similar curves with Fig. 5(a) are given in Fig. 5(b) but for the application of the advanced FIIM. Similar curves with Figs. 5(a) and 5(b) are given in Figs. 5(c) and 5(d) for the suburban case and in Figs. 5(e) and 5(f) for the rural case.

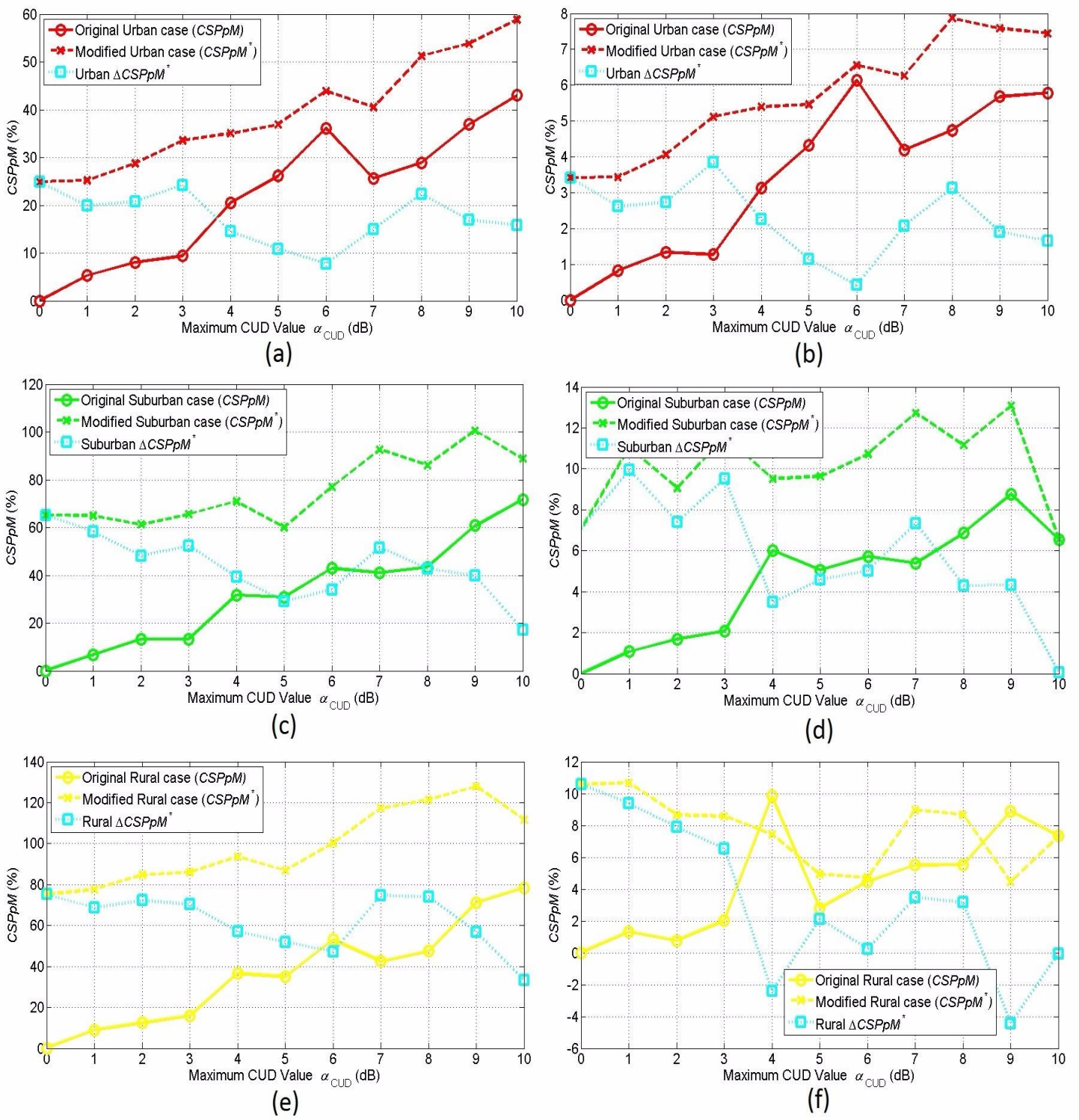

Figure 5. Instability in the branch interconnection of the last branch of the indicative OV MV BPL topologies and the behavior of CSPpMs and ΔCSPpM*. (a) FIIM / Urban case. (b) Advanced FIIM / Urban case. (c) FIIM / Suburban case. (d) Advanced FIIM / Suburban case. (e) FIIM / Rural case. (f) Advanced FIIM / Rural case.

From Figs. 5(a)-(f), $\Delta CSPpM^*$ of FIIM and advanced FIIM can identify the branch interconnection instability regardless of the considered OV MV BPL topology and the applied CUD magnitude. Although the identification of the branch interconnection instability becomes more challenging as the maximum CUD value increases, $\Delta CSPpM^*$ triggers the alarm in all the cases examined except for the application of FIIM in rural case when maximum CUD value exceeds 9dB. Therefore, FIIM and advanced FIIM present almost the same identification performance of a branch interconnection instability but advanced FIIM is characterized by better execution times.

4.4.4 Instability in Branch Terminations

This subsection examines the possibility of identifying an instability that occurs in a branch termination. With reference to Fig. 1(e), let the branch termination of the first branch of each indicative OV MV BPL topology act as short circuit termination. This short circuit at the first branch termination may come up from a short circuit inside a MV/LV transformer. FIIM and advanced FIIM can identify the instability in branch terminations by applying $\Delta CSPpM^*$. Similarly to branch line faults and branch interconnection instabilities, in Fig. 6(a), CSPpM of the original urban OV MV BPL topology, CSPpM* of the modified urban OV MV BPL topology and their $\Delta CSPpM^*$ are plotted versus the CUD maximum value of the occurred measurement differences when FIIM is applied. Similar curves with Fig. 6(a) are given in Fig. 6(b) but for the application of the advanced FIIM. Similar curves with Figs. 6(a) and 6(b) are given in Figs. 6(c) and 6(d) for the suburban case and in Figs. 5(e) and 5(f) for the rural case.

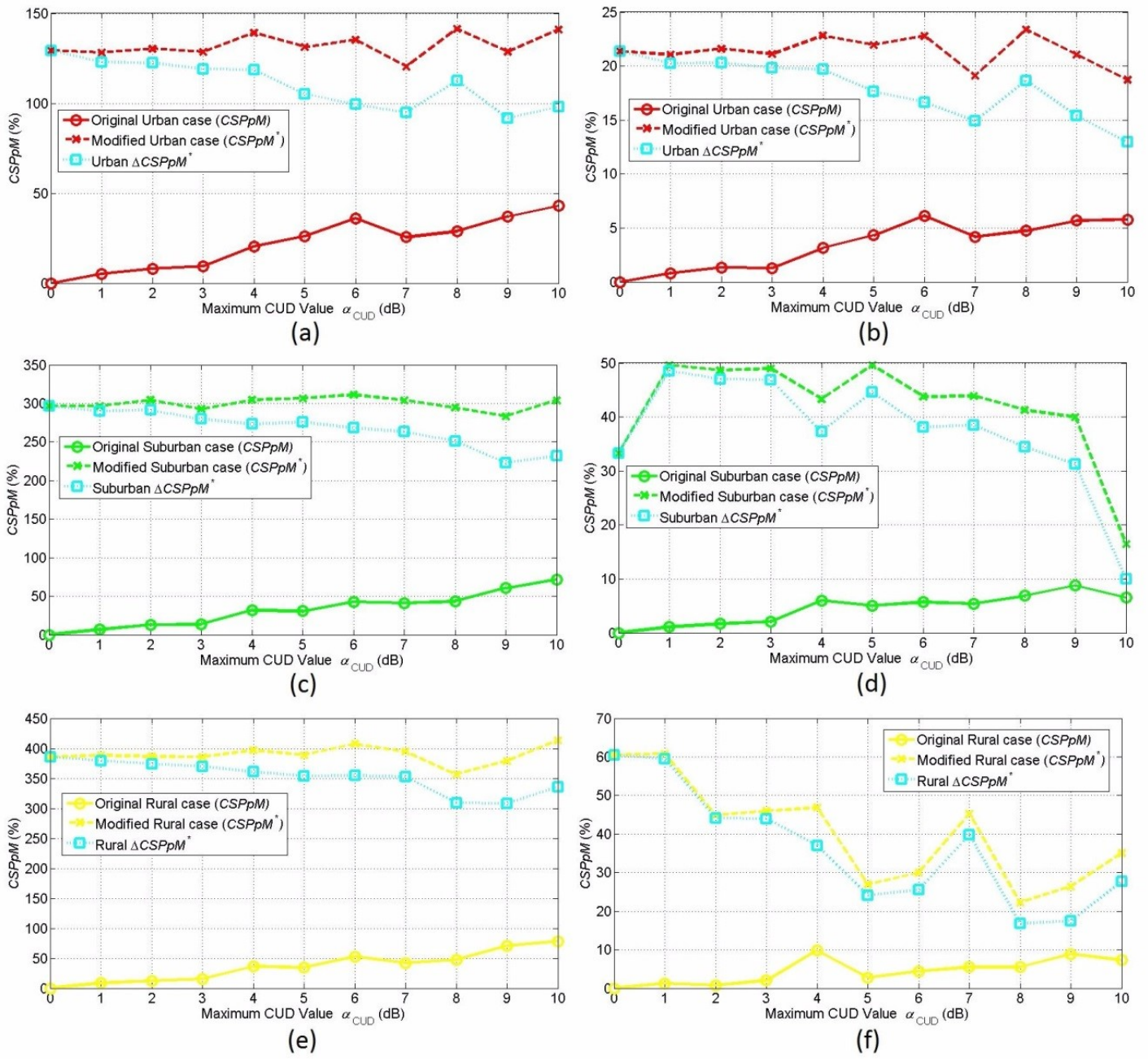

Figure 6. Instability in the branch termination (short circuit) of the first branch of the indicative OV MV BPL topologies and the behavior of CSPpMs and ΔCSPpM*. (a) FIIM / Urban case. (b) Advanced FIIM / Urban case. (c) FIIM / Suburban case. (d) Advanced FIIM / Suburban case. (e) FIIM / Rural case. (f) Advanced FIIM / Rural case.

From Figs. 6(a)-(f), both FIIM and advanced FIIM can easily identify any damage that may affect pieces of equipment across the distribution power grid. This is clear from the comparison among the previous figures where various faults and instabilities occur. In the case of the short circuit termination, there is not only one case where $\Delta CSPpM^*$ lies below 0dB. The identification of the instability remains easy even if high maximum CUD values are encountered that exceed 6-7dB. Again, FIIM and advanced FIIM present almost the same identification performance of a branch termination instability but advanced FIIM is characterized by better execution times.

4.5 General Remarks Regarding TIM, Advanced TIM, FIIM and Advanced FIIM

Already been mentioned in [24], [25], TIM, advanced TIM, FIIM and advanced FIIM can act as invaluable smart grid applications towards the power stability of the transmission and power grids.

Among the research goals that have been presented in [25], advanced TIM and advanced FIIM can successfully cope with the challenges of the BPL topology identification as well as the fault and instability identification. Actually, advanced TIM performance towards the identification of OV MV BPL topologies remains almost the same with TIM, as described in Figs. 2(a), 2(b), 3(a) and 3(b), but reducing significantly the approximated time duration as well as the complicacy of the examined OV MV BPL topologies. In accordance with Table 2, the key of advanced TIM that allows the reduction of the approximated time duration is the adoption of the concept of the adaptive number of monotonic sections presented in [27] when the required OV MV BPL topology database is prepared. Similarly to advanced TIM, advanced FIIM performance remains almost the same with FIIM when the problematic conditions of Secs. 4.4.1-4.4.4 occur. Again, advanced FIIM execution time is drastically reduced comparing with the respective time of FIIM.

5. Conclusions

In this paper, TIM and FIIM have first applied to distribution power grids while the respective advanced TIM and advanced FIIM have been proposed.

As the validation of the TIM and advanced TIM are concerned, a set of candidate OV MV BPL topologies has been revealed with the real original topology lying inside the set by using the TIM performance metric of $CSPM_{tot}$. Even though measurement differences of various maximum CUD values have been assumed, TIM and advanced TIM have satisfactorily achieved to identify the real original topology with almost the same accuracy. However, advanced TIM succeeds in identifying original OV MV BPL topologies with significant shorter execution times in comparison with TIM.

As regards the validation of the FIIM and advanced FIIM, four problematic conditions (i.e., faults in main distribution lines, faults in branch lines, instabilities in branch interconnections and instabilities in branch terminations) have been easily identified. Through FIIM performance metric of $\Delta CSPpM^*$, FIIM and advanced FIIM have successfully managed to identify the four problematic conditions. Again, advanced FIIM presents significantly shorter execution times when OV MV BPL topologies are examined in comparison with FIIM.

Exploiting the virtues of the emerging intelligent energy systems, advanced TIM and FIIM complete another step towards the real time surveillance and monitoring of transmission and distribution power grid.

References

[1] K. Ali, I. Pefkianakis, A. X. Liu, and K. H. Kim, "Boosting PLC Networks for High-Speed Ubiquitous Connectivity in Enterprises," arXiv preprint arXiv:1608.06574, 2016, [Online]. Available: http://arxiv.org/pdf/1608.06574v1.pdf

[2] A. G. Lazaropoulos, "Best L1 Piecewise Monotonic Data Approximation in Overhead and Underground Medium-Voltage and Low-Voltage Broadband over Power Lines Networks: Theoretical and Practical Transfer Function Determination," *Hindawi Journal of Computational Engineering*, vol. 2016, Article ID 6762390, 24 pages, 2016. DOI:10.1155/2016/6762390. [Online]. Available: https://www.hindawi.com/journals/jcengi/2016/6762390/cta/

[3] C. Cano, A.Pittolo, D. Malone, L. Lampe, A. M.Tonello, and A. Dabak, "State-of-the-art in Power Line Communications: From the Applications to the Medium," *IEEE J. Sel. Areas Commun.*,vol. 34, pp. 1935-1952, 2016.

[4] L. Lampe, A. M. Tonello, and T. G. Swart, *Power Line Communications: Principles, Standards and Applications from Multimedia to Smart Grid*. John Wiley & Sons, 2016.

[5] A. G. Lazaropoulos and P. G. Cottis, "Transmission characteristics of overhead medium voltage power line communication channels," *IEEE Trans. Power Del.*, vol. 24, no. 3, pp. 1164-1173, Jul. 2009.

[6] A. G. Lazaropoulos and P. G. Cottis, "Capacity of overhead medium voltage power line communication channels," *IEEE Trans. Power Del.*, vol. 25, no. 2, pp. 723-733, Apr. 2010.

[7] A. G. Lazaropoulos and P. G. Cottis, "Broadband transmission via underground medium-voltage power lines-Part I: transmission characteristics," *IEEE Trans. Power Del.*, vol. 25, no. 4, pp. 2414-2424, Oct. 2010.

[8] A. G. Lazaropoulos and P. G. Cottis, "Broadband transmission via underground medium-voltage power lines-Part II: capacity," *IEEE Trans. Power Del.*, vol. 25, no. 4, pp. 2425-2434, Oct. 2010.

[9] A. G. Lazaropoulos, "Broadband transmission characteristics of overhead high-voltage power line communication channels," *Progress in Electromagnetics Research B*, vol. 36, pp. 373-398, 2012. [Online]. Available: http://www.jpier.org/PIERB/pierb36/19.11091408.pdf

[10] A. G. Lazaropoulos, "Capacity Performance of Overhead Transmission Multiple-Input Multiple-Output Broadband over Power Lines Networks: The Insidious Effect of Noise and the Role of Noise Models," *Trends in Renewable Energy*, vol. 2, no. 2, pp. 61-82, Jan. 2016. DOI: 10.17737/tre.2016.2.2.0023

[11] Homeplug, Technology Gains Momentum, 2013, [Online]. Available: http://www.businesswire.com

[12] Homeplug, AVWhitepaper, 2007, [Online]. Available: http://www.homeplug.org/techresources/resources/

[13] Homeplug, AV2Whitepaper, 2011, [Online]. Available: http://www.homeplug.org/techresources/resources/

[14] A. G. Lazaropoulos, "Factors Influencing Broadband Transmission Characteristics of Underground Low-Voltage Distribution Networks," *IET Commun.*, vol. 6, no. 17, pp. 2886-2893, Nov. 2012.

[15] A. G. Lazaropoulos, "Towards broadband over power lines systems integration: Transmission characteristics of underground low-voltage distribution power lines," *Progress in Electromagnetics Research B*, 39, pp. 89-114, 2012. [Online]. Available: http://www.jpier.org/PIERB/pierb39/05.12012409.pdf

[16] A. G. Lazaropoulos, "Broadband transmission and statistical performance properties of overhead high-voltage transmission networks,"*Hindawi Journal of Computer Networks and Commun.*, 2012, article ID 875632, 2012. [Online]. Available: http://www.hindawi.com/journals/jcnc/aip/875632/

[17] A. G. Lazaropoulos, "Towards modal integration of overhead and underground low-voltage and medium-voltage power line communication channels in the smart grid landscape: model expansion, broadband signal transmission characteristics, and statistical performance metrics (Invited Paper)," *ISRN Signal Processing*, vol. 2012, Article ID 121628, 17 pages, 2012. [Online]. Available: http://www.isrn.com/journals/sp/aip/121628/

[18] A. G. Lazaropoulos, "Review and Progress towards the Common Broadband Management of High-Voltage Transmission Grids: Model Expansion and Comparative Modal Analysis," *ISRN Electronics*, vol. 2012, Article ID 935286, pp. 1-18, 2012. [Online]. Available: http://www.hindawi.com/isrn/electronics/2012/935286/

[19] A. G. Lazaropoulos, "Review and Progress towards the Capacity Boost of Overhead and Underground Medium-Voltage and Low-Voltage Broadband over Power Lines Networks: Cooperative Communications through Two- and Three-Hop Repeater Systems," *ISRN Electronics*, vol. 2013, Article ID 472190, pp. 1-19, 2013. [Online]. Available: http://www.hindawi.com/isrn/electronics/aip/472190/

[20] A. G. Lazaropoulos, "Green Overhead and Underground Multiple-Input Multiple-Output Medium Voltage Broadband over Power Lines Networks: Energy-Efficient Power Control," *Springer Journal of Global Optimization*, vol. 2012 / Print ISSN 0925-5001, pp. 1-28, Oct. 2012.

[21] P. Amirshahi and M. Kavehrad, "High-frequency characteristics of overhead multiconductor power lines for broadband communications," *IEEE J. Sel. Areas Commun.*, vol. 24, no. 7, pp. 1292-1303, Jul. 2006.

[22] T. Sartenaer, "Multiuser communications over frequency selective wired channels and applications to the powerline access network," Ph.D. dissertation, Univ. Catholique Louvain, Louvain-la-Neuve, Belgium, Sep. 2004.

[23] T. Calliacoudas and F. Issa, ""Multiconductor transmission lines and cables solver," An efficient simulation tool for plc channel networks development," presented at the *IEEE Int. Conf. Power Line Communications and Its Applications*, Athens, Greece, Mar. 2002.

[24] A. G. Lazaropoulos, "Measurement Differences, Faults and Instabilities in Intelligent Energy Systems – Part 1: Identification of Overhead High-Voltage Broadband over Power Lines Network Topologies by Applying Topology Identification Methodology (TIM)," *Trends in Renewable Energy*, vol. 2, no. 3, pp. 85 – 112, Oct. 2016. DOI: 10.17737/tre.2016.2.3.0026

[25] A. G. Lazaropoulos, "Measurement Differences, Faults and Instabilities in Intelligent Energy Systems – Part 2: Fault and Instability Prediction in Overhead High-Voltage Broadband over Power Lines Networks by Applying Fault and Instability Identification Methodology (FIIM)," *Trends in Renewable Energy*, vol. 2, no. 3, pp. 113 – 142, Oct. 2016. DOI: 10.17737/tre.2016.2.3.0027

[26] A. G. Lazaropoulos, "Power Systems Stability through Piecewise Monotonic Data Approximations – Part 1: Comparative Benchmarking of L1PMA, L2WPMA and L2CXCV in Overhead Medium-Voltage Broadband over Power Lines Networks," *Trends in Renewable Energy*, vol. 3, no. 1, pp. 2 – 32, Jan. 2017. DOI: 10.17737/tre.2017.3.1.0029

[27] A. G. Lazaropoulos, "Power Systems Stability through Piecewise Monotonic Data Approximations – Part 2: Adaptive Number of Monotonic Sections and Performance of L1PMA, L2WPMA and L2CXCV in Overhead Medium-Voltage Broadband over Power Lines Networks," *Trends in Renewable Energy*, vol. 3, no. 1, pp. 33 – 60, Jan. 2017. DOI: 10.17737/tre.2017.3.1.0030

[28] P. Amirshahi, "Broadband access and home networking through powerline networks" Ph.D. dissertation, Pennsylvania State Univ., University Park, PA, May 2006. [Online]. Available: http://etda.libraries.psu.edu/theses/approved/WorldWideIndex/ETD-1205/index.html

[29] M. D'Amore and M. S. Sarto, "Simulation models of a dissipative transmission line above a lossy ground for a wide-frequency range-Part I: Single conductor configuration," *IEEE Trans. Electromagn. Compat.*, vol. 38, no. 2, pp. 127-138, May 1996.

[30] M. D'Amore and M. S. Sarto, "Simulation models of a dissipative transmission line above a lossy ground for a wide-frequency range-Part II: Multi-conductor configuration," *IEEE Trans. Electromagn. Compat.*, vol. 38, no. 2, pp. 139-149, May 1996.

[31] A. Milioudis, G. T. Andreou, and D. P. Labridis, "Detection and location of high impedance faults in multiconductor overhead distribution lines using power line communication devices," *IEEE Trans. on Smart Grid*, vol. 6, no. 2, pp. 894-902, 2015.

[32] A. G. Lazaropoulos, "Designing Broadband over Power Lines Networks Using the Techno-Economic Pedagogical (TEP) Method – Part I: Overhead High Voltage Networks and Their Capacity Characteristics (Invited Review Article)," *Trends in Renewable Energy*, vol. 1, no. 1, pp. 16-42, Mar. 2015. DOI: 10.17737/tre.2015.1.1.002

[33] A. G. Lazaropoulos, "Designing Broadband over Power Lines Networks Using the Techno-Economic Pedagogical (TEP) Method – Part II: Overhead Low-Voltage and Medium-Voltage Channels and Their Modal Transmission Characteristics," *Trends in Renewable Energy*, vol. 1, no. 2, pp. 59-86, Jun. 2015. DOI: 10.17737/tre.2015.1.2.006

[34] T. Sartenaer and P. Delogne, "Deterministic modelling of the (Shielded) outdoor powerline channel based on the multiconductor transmission line equations," *IEEE J. Sel. Areas Commun.*, vol. 24, no. 7, pp. 1277-1291, Jul. 2006.

[35] A. G. Lazaropoulos, "Policies for Carbon Energy Footprint Reduction of Overhead Multiple-Input Multiple-Output High Voltage Broadband over Power

Lines Networks," *Trends in Renewable Energy*, vol. 1, no. 2, pp. 87-118, Jun. 2015. DOI: 10.17737/tre.2015.1.2.0011

[36] A. G. Lazaropoulos, "Wireless Sensor Network Design for Transmission Line Monitoring, Metering and Controlling: Introducing Broadband over PowerLines-enhanced Network Model (BPLeNM)," *ISRN Power Engineering*, vol. 2014, Article ID 894628, 22 pages, 2014. DOI: 10.1155/2014/894628. [Online]. Available: http://www.hindawi.com/journals/isrn.power.engineering/2014/894628/

[37] A. G. Lazaropoulos, "Wireless Sensors and Broadband over PowerLines Networks: The Performance of Broadband over PowerLines-enhanced Network Model (BPLeNM) (Invited Paper)," *ICAS Publishing Group Transaction on IoT and Cloud Computing*, vol. 2, no. 3, pp. 1-35, 2014. [Online]. Available: http://icas-pub.org/ojs/index.php/ticc/article/view/27/17

[38] A. G. Lazaropoulos, "The Impact of Noise Models on Capacity Performance of Distribution Broadband over Power Lines (BPL) Networks," *Hindawi Computer Networks and Communications*, vol. 2016, Article ID 5680850, 14 pages, 2016. doi:10.1155/2016/5680850. [Online]. Available: http://www.hindawi.com/journals/jcnc/2016/5680850/

[39] I. C. Demetriou and M. J. D. Powell, "Least squares smoothing of univariate data to achieve piecewise monotonicity,"*IMA J. of Numerical Analysis*, vol. 11, pp. 411-432, 1991.

[40] I. C. Demetriou and V. Koutoulidis, "On Signal Restoration by Piecewise Monotonic Approximation", in Lecture Notes in Engineering and Computer Science: *Proceedings of The World Congress on Engineering 2013*,London, U.K., Jul. 2013, pp. 268-273.

[41] I. C. Demetriou, "An application of best *L*1 piecewise monotonic data approximation to signal restoration," *IAENG International Journal of Applied Mathematics*, vol. 53, no. 4, pp. 226-232, 2013.

[42] I. C. Demetriou, "L1PMA: A Fortran 77 Package for Best L1 Piecewise Monotonic Data Smoothing," *Computer Physics Communications*, vol. 151, no. 1, pp. 315-338, 2003.

[43] I. C. Demetriou, "Data Smoothing by Piecewise Monotonic Divided Differences,"*Ph.D. Dissertation*, Department of Applied Mathematics and Theoretical Physics, University of Cambridge, Cambridge, 1985.

[44] I. C. Demetriou, "Best L1 Piecewise Monotonic Data Modelling,"*Int. Trans. Opl Res.*, vol. 1, no. 1, pp. 85-94,1994.